Short Papers

Berenger and Leaky Modes in Microstrip Substrates Terminated by a Perfectly Matched Layer

Hendrik Rogier and Daniël De Zutter

***Abstract*—In this paper, it is shown that the dispersion relation of a microstrip substrate terminated by a perfectly matched layer (PML) allows two sets of zeros. For a strongly absorbing PML, the first set does not depend on the characteristics of that layer. Within a good approximation, it corresponds to the leaky modes of the microstrip substrate. The second set is not influenced by the microstrip substrate. Since it mainly depends on the characteristics of the PML, this set of modes are called the Berenger modes. Analytic expressions are derived for these two sets of zeros in the quasi-static limit.**

***Index Terms*—Absorbing media, dielectric load waveguides, Green's function, leaky waves, microstrip.**

I. Introduction

A perfectly matched layer (PML), as introduced by Berenger [1], combines as good absorption of electromagnetic fields in the direction perpendicular to the layer with a good phase matching at the interface between the PML and adjacent medium. This can either be achieved by a suitable choice of uniaxial anisotropic material parameters for the PML [2] or by stretching the coordinates in Maxwell's equations [3], [4].

Besides its usefulness as an excellent absorbing boundary condition in finite-element and finite-difference time-domain scattering codes, PMLs can also be applied to perform efficient calculations in waveguide configurations. The PML then mimics an open configuration, while an efficient problem description in terms of a set of discrete modes of the closed waveguide containing the PML is possible [5], [6]. A key issue in this approach is the knowledge of the eigenvalues β and eigenmode profiles pertaining to the PML waveguide configuration.

In this paper, we will discuss some properties of the eigenmodes that can exist in two-dimensional (2-D) waveguides formed by a microstrip substrate terminated by a PML. For a strongly absorbing PML, the solution of the dispersion relation allows two sets of zeros. It is shown that one set corresponds to the leaky modes of the microstrip substrate, while the second set mainly depends on the characteristics of the PML. For both sets of eigenvalues, analytic approximations can be derived in the quasi-static limit. In Section II, the properties of the TE modes are discussed, while in Section III, TM modes are discussed. Finally, the theoretical results are illustrated by numerical data in Section IV.

II. Theory—TE Modes

Consider the configuration shown in Fig. 1, consisting of a microstrip substrate with permittivity ϵ_r, permeability μ_r, and thickness d. Above the substrate, an air region is present with thickness $d_{\rm air}$, terminated by a PML with thickness $d_{\rm PML}$ and with material parameters κ_0 and σ_0 [5]. In [7], it is shown that, by stretching the coordinates, the air region can be combined with the PML to form a single air layer with complex thickness $\tilde{d} = d_{\rm air} + d_{\rm PML}(\kappa_0 - j(\sigma_0/\omega\epsilon_0))$. This allows a relatively simple modal analysis of the waveguide under consideration.

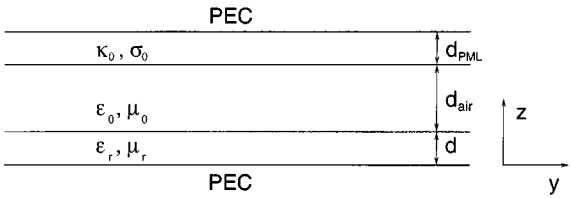

Fig. 1. Microstrip configuration.

For modes propagating in the y-direction with propagation constant β, the TE eigenmode profiles of the configuration are given by

$$E_x(y,z) = \begin{cases} A\sin(\gamma_r z)\sin\left(\gamma_0 \tilde{d}\right) e^{-j\beta y}, & 0 < z < d \\ A\sin(\gamma_r d)\sin\left[\gamma_0\left(\tilde{d} + d - z\right)\right] e^{-j\beta y}, & d < z < d + d_{\rm air} \end{cases} \tag{1}$$

with A being a normalization factor and γ_r and γ_0 satisfying

$$Y_r \cot(\gamma_r d) = -Y_0 \cot\left(\gamma_0 \tilde{d}\right) \tag{2}$$

with $\gamma_0^2 = k_0^2 - \beta^2$, $\gamma_r^2 = k_0^2\epsilon_r\mu_r - \beta^2$, $Y_r = \gamma_r/\mu_0\mu_r$ and $Y_0 = \gamma_0/\mu_0$, and $k_0^2 = \omega^2\epsilon_0\mu_0$. To assure propagation in the $+y$-direction with a bounded mode profile, the propagation constants must obey $\mathrm{Re}(\beta) \geq 0$ and $\mathrm{Im}(\beta) \leq 0$. Branch cuts are then chosen so that $\mathrm{Re}(\gamma_r), \mathrm{Re}(\gamma_0) \geq 0$, and $\mathrm{Im}(\gamma_r), \mathrm{Im}(\gamma_0) \geq 0$.

We will now concern ourselves with the solution of the dispersion relation (2). This expression can be rewritten as

$$e^{-2j\gamma_r d} = \frac{Y_r + Y_0 + (Y_0 - Y_r)e^{-2j\gamma_0\tilde{d}}}{Y_0 - Y_r + (Y_r + Y_0)e^{-2j\gamma_0\tilde{d}}}. \tag{3}$$

No simple analytical solutions for the eigenvalues β can be found for (2). However, when the PML acts as a strong absorber, some approximations can be made in order to simplify the dispersion relations. We will distinguish between the following two particular cases.

1) For the first set of modes, we assume that most of the modal field is concentrated in the microstrip substrate, while the PML strongly attenuates the field. This corresponds to the assumption that $|\mathrm{Re}(\gamma_0)|d_{\rm PML}(\sigma_0/\omega\epsilon_0)$ is large and that $|\mathrm{Im}(\gamma_0)| \ll (d_{\rm PML}(\sigma_0/\omega\epsilon_0)/(d_{\rm air} + d_{\rm PML}\kappa_0))|\mathrm{Re}(\gamma_0)|$. We then have $|e^{-2j\gamma_0\tilde{d}}| \ll 1$; this is the case of a perfect absorbing boundary condition. The problem reduces to the classical microstrip substrate, for which the dispersion relation is given by

$$Y_r \cot(\gamma_r d) = -jY_0. \tag{4}$$

For $\mathrm{Re}(\gamma_0) > 0$, (2) can be rewritten as

$$e^{-2j\gamma_r d} = \frac{Y_r + Y_0}{Y_0 - Y_r}. \tag{5}$$

The solutions of this equation in the complex plane are known as the leaky modes of the microstrip substrate.

Manuscript received June 9, 2000; revised August 4, 2000.

The authors are with the Information Technology Department, Ghent University, B-9000 Ghent, Belgium (e-mail: hendrik.rogier@intec.rug.ac.be; daniel.dezutter@intec.rug.ac.be).

Publisher Item Identifier S 0018-9480(01)02420-6.

2) For the second set of modes, we assume that most of the modal field is concentrated in the PML, while a strong attenuation is found in the microstrip substrate. This is satisfied when $|\mathrm{Im}(\gamma_r)|d$ is large, implying that $|e^{+2j\gamma_r d}| \ll 1$; thus, (2) can be written as

$$e^{-2j\gamma_0 \tilde{d}} = \frac{Y_r - Y_0}{Y_r + Y_0}. \tag{6}$$

Since the behavior of this type of modes mainly depends on the characteristics of the PML, we will call them Berenger modes.

We will now look for analytic solutions for the propagation constants of the leaky and Berenger modes in the quasi-static limit. The assumption that $\omega\sqrt{\epsilon_0\mu_0} \ll \beta$ allows the approximation

$$\gamma_r \approx \gamma_0 \approx +j\beta. \tag{7}$$

A. Leaky Modes

Equation (5) can be written as

$$e^{2j\gamma_r d} = k_0^2 \frac{\mu_r^2 - \mu_r\epsilon_r}{(\gamma_0\mu_r + \gamma_r)^2} - \beta^2 \frac{\mu_r^2 - 1}{(\gamma_0\mu_r + \gamma_r)^2}. \tag{8}$$

Applying the quasi-static approximation (7) yields

$$e^{2j\gamma_r d} = \frac{k_0^2}{\gamma_r^2} \frac{\mu_r^2 - \mu_r\epsilon_r}{(\mu_r + 1)^2} + \frac{\mu_r - 1}{\mu_r + 1}. \tag{9}$$

If one assumes that $\mu_r \neq 1$, this equation is satisfied by

$$+j\beta \approx \gamma_r \approx \frac{1}{2jd} \log\left|\frac{\mu_r - 1}{\mu_r + 1}\right| + \frac{n\pi}{d}. \tag{10}$$

For $\mu_r = 1$, (8) reduces to

$$e^{2j\gamma_r d} = \frac{k_0^2}{\gamma_r^2} \frac{1 - \epsilon_r}{4}. \tag{11}$$

Closed-form solutions of this equation can be found under the form of Lambert W [8] functions

$$+j\beta \approx \gamma_r \approx -\frac{j}{d}\text{Lambert W}\left(m, \pm\frac{1}{2}k_0 d\sqrt{\epsilon_r - 1}\right). \tag{12}$$

The zeros can be approximated by

$$+j\beta \approx \gamma_r \approx \frac{(2n+1)\pi}{2d} + j\frac{1}{d}\log\frac{(2n+1)\pi}{k_0 d\sqrt{\epsilon_r - 1}}. \tag{13}$$

B. Berenger Modes

Under quasi-static approximation (7) and for $\mu_r \neq 1$, (6) reduces to

$$e^{-2j\gamma_0 \tilde{d}} = \frac{1 - \mu_r}{1 + \mu_r}. \tag{14}$$

For $\mu_r \neq 1$, the zeros that characterize the Berenger modes are easily found by

$$+j\beta \approx \gamma_0 \approx -\frac{1}{2j\tilde{d}} \log\left|\frac{\mu_r - 1}{\mu_r + 1}\right| + \frac{(2n+1)\pi}{2\tilde{d}}. \tag{15}$$

In the particular case of no magnetic contrasts and for $\epsilon_r \neq 1$, (6) reduces to

$$e^{-2j\gamma_0 \tilde{d}} = \frac{k_0^2(\epsilon_r - 1)}{4\gamma_0^2} \tag{16}$$

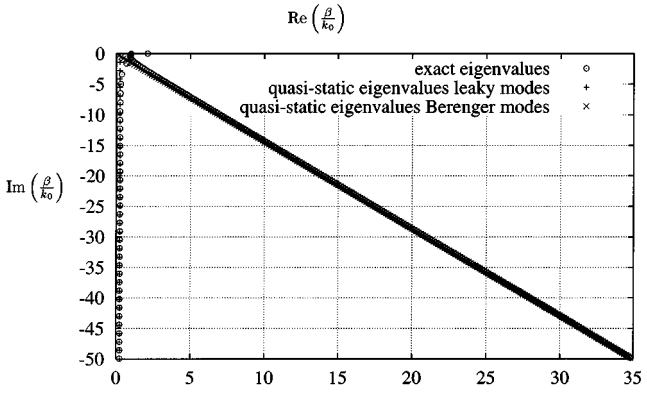

Fig. 2. Location of the eigenvalues β/k_0 of the TE modes for a microstrip–PML configuration with magnetic contrast.

TABLE I
LOCATION OF SOME EIGENVALUES β/k_0 OF LEAKY MODES

n (10)	quasi-static eigenvalue (10)	exact eigenvalue
10	0.242846-j13.888889	0.250684-j13.671399
15	0.242846-j20.833333	0.246270-j20.688893
20	0.242846-j27.777778	0.244760-j27.669592
25	0.242846-j34.722222	0.244068-j34.635727
30	0.242846-j41.666667	0.243694-j41.594612

TABLE II
LOCATION OF SOME EIGENVALUES β/k_0 OF BERENGER MODES

n (15)	quasi-static eigenvalue (15)	exact eigenvalue
20	2.972975-j4.325166	3.023709-j4.244097
40	5.909215-j8.519796	5.935769-j8.479484
60	8.845455-j12.714426	8.863462-j12.687615
80	11.781695-j16.909056	11.795322-j16.888975
100	14.717935-j21.103686	14.728898-j21.087635

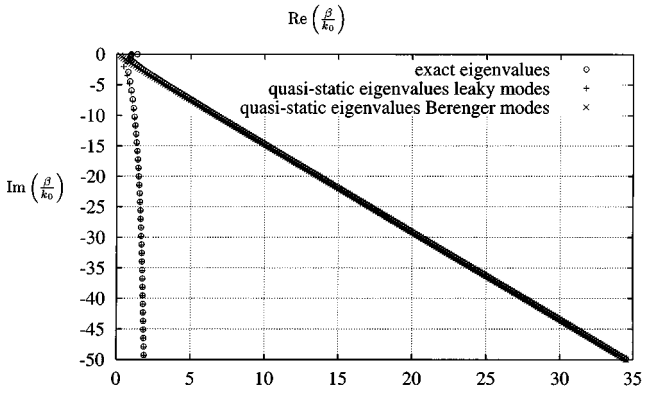

Fig. 3. Location of the eigenvalues β/k_0 of the TE modes for a microstrip–PML configuration without magnetic contrast.

TABLE III
LOCATION OF SOME EIGENVALUES β/k_0 OF LEAKY MODES

n (13)	quasi-static eigenvalue (13)	quasi-static eigenvalue (12)	exact eigenvalue
10	1.337986-j14.583333	1.338619-j14.542753 ($m = 5$, -)	1.347096-j14.439964
15	1.510167-j21.527778	1.510618-j21.496761 ($m = 8$, +)	1.515046-j21.427159
20	1.633771-j28.472222	1.634104-j28.446854 ($m = 10$, -)	1.636861-j28.394223
25	1.730260-j35.416667	1.730518-j35.395069 ($m = 13$, +)	1.732413-j35.352751
30	1.809417-j42.361111	1.809623-j42.342228 ($m = 15$, -)	1.811013-j42.306843

TABLE IV
LOCATION OF SOME EIGENVALUES β/k_0 OF BERENGER MODES

n (18)	quasi-static eigenvalue (18)	quasi-static eigenvalue (17)	exact eigenvalue
20	2.832825-j4.327772	2.830502-j4.326278 ($m = 10$, -)	2.883047-j4.244715
40	5.722792-j8.554795	5.721262-j8.553756 ($m = 20$, -)	5.748065-j8.513185
60	8.631965-j12.768374	8.630773-j12.767587 ($m = 30$, -)	8.648833-j12.740622
80	11.549001-j16.976449	11.548000-j16.975819 ($m = 40$, -)	11.561632-j16.955634
100	14.470346-j21.181508	14.469469-j21.180986 ($m = 50$, -)	14.480420-j21.164859

in the quasi-static limit. Closed-form solutions of this equation also exist under the form of Lambert W functions

$$+j\beta \approx \gamma_0 \approx \frac{j}{\tilde{d}}\text{Lambert W}\left(-m,\ \pm j\frac{1}{2}\,k_0\tilde{d}\sqrt{\epsilon_r - 1}\right). \tag{17}$$

The zeros can be approximated by

$$+j\beta \approx \gamma_0 \approx \frac{n\pi}{\tilde{d}} - j\frac{1}{\tilde{d}}\log\frac{2n\pi}{k_0\,\tilde{d}\sqrt{\epsilon_r - 1}}. \tag{18}$$

III. THEORY—TM MODES

The TM eigenmode profiles of the waveguide shown in Fig. 1 are given by

$$H_x(y,\ z) = \begin{cases} A\cos(\gamma_r z)\cos\left(\gamma_0\tilde{d}\right)e^{-j\beta y}, & 0 < z < d \\ A\cos(\gamma_r d)\cos\left[\gamma_0\left(\tilde{d} + d - z\right)\right]e^{-j\beta y}, & d < z < d + d_{\text{air}} \end{cases} \tag{19}$$

with γ_r and γ_0 satisfying

$$Y_r\cot(\gamma_r d) = -Y_0\cot\left(\gamma_0\tilde{d}\right) \tag{20}$$

with $Y_r = \epsilon_r\epsilon_0/\gamma_r$ and $Y_0 = \epsilon_0/\gamma_0$.

Following the same line of reasoning as in Section II, one can again distinguish between leaky modes, depending on the microstrip substrate, and Berenger modes, mainly influenced by the PML. For $\epsilon_r \neq 1$, one finds the following closed-form expression for the leaky mode solution in the quasi-static limit:

$$\gamma = \frac{1}{2jd}\log\left|\frac{\epsilon_r - 1}{\epsilon_r + 1}\right| + \frac{(2n+1)\pi}{2d}. \tag{21}$$

As for the Berenger modes, the following solution is found:

$$\gamma_0 = -\frac{1}{2j\tilde{d}}\log\left|\frac{\epsilon_r - 1}{\epsilon_r + 1}\right| + \frac{n\pi}{\tilde{d}}. \tag{22}$$

IV. EXAMPLES

In order to illustrate the theory developed in the previous sections, we consider a microstrip–PML configuration with $d = 9$ mm, $d_{\text{air}} = 5$ mm, and $d_{\text{PML}} = 3.5$ mm at 12 GHz. A strongly absorbing PML is obtained for $\kappa_0 = 10$ and $\sigma_0/\omega\epsilon_0 = 8$. Let us first study a microstrip substrate with magnetic and electric contrasts, choosing, e.g., $\epsilon_r = 3$ and $\mu_r = 2$. In Fig. 2, the propagation constants of the TE modes are shown. Besides the exact locations of the normalized modal constants obtained with a numerical root-solving routine, the quasi-static eigenvalues is given, following the analytic formulas (10) and (15), which were derived under the assumption (7). For increasing magnitudes of β, the analytic expressions (10) and (15), respectively, for the leaky and Berenger modes, are seen to convergence to the exact locations of the normalized modal constants β/k_0, as illustrated in Tables I and II. Compared to the exact eigenvalue for the leaky modes, (10) yields values with a 1% relative accuracy for $n > 12$. For the Berenger modes, a 1% relative accuracy is obtained with (15) for $n > 27$.

In Fig. 3, the propagation constants of the TE modes are shown, when there are no magnetic contrasts, i.e., when $\epsilon_r = 3$ and $\mu_r = 1$. The exact locations of the normalized modal constants obtained with a numerical root-solving routine are compared to the quasi-static eigenvalues, following the analytic formulas (13) and (18), which were derived under assumption (7). Again, good agreement is seen between the exact locations of the eigenvalues and the β values obtained with the analytic expressions (13) and (18) whenever β becomes large, as compared to k_0, as demonstrated in Tables III and IV. Compared to the exact eigenvalue for the leaky modes, (13) yields values with a 1% relative accuracy for $n > 10$. For the Berenger modes, a 1% relative accuracy is obtained with (18) for $n > 27$. Similar observations hold for the propagation constants of the TM modes, as demonstrated in Fig. 4.

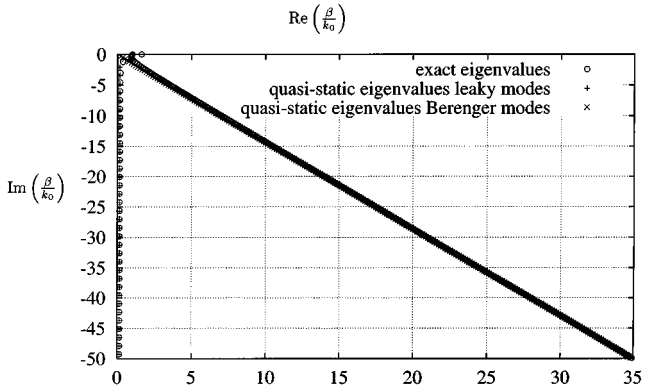

Fig. 4. Location of the eigenvalues β/k_0 of the TM modes for a microstrip–PML configuration.

V. Conclusions

Analytic expressions in the quasi-static limit are derived for two sets of zeros, which exist in a microstrip substrate terminated by a PML. For a strongly absorbing PML, it is shown that the first set corresponds to the leaky modes of the microstrip substrate, whereas the second set, termed Berenger modes, is not influenced by the microstrip substrate. As demonstrated by examples, the analytical formulas allow a quick calculation of the modal constants whenever $\omega\sqrt{\epsilon_0\mu_0} \ll \beta$. Moreover, the quasi-static expressions can be used as initial guesses in a numerical root-finding routine that can provide more accurate values for the zeros of the dispersion relation. Thereby, our results can speed up the calculation of the Green's function of the microstrip substrate terminated by a PML, as discussed in [5].

References

[1] J. P. Berenger, "Perfectly matched layer for the FDTD solution of wave-structure interaction problems," *IEEE Trans. Antennas Propagat.*, vol. 44, pp. 110–117, Jan. 1996.

[2] S. D. Gedney, "An anisotropic PML absorbing media for the FDTD simulation of fields in lossy and dispersive media," *Electromag.*, vol. 16, pp. 399–415, 1996.

[3] W. C. Chew and W. H. Weedon, "A 3D perfectly matched medium from modified Maxwell's equations in stretched coordinates," *Microwave Opt. Technol. Lett.*, vol. 7, no. 13, pp. 599–604, Sept. 1994.

[4] L. Knockaert and D. De Zutter, "On the stretching of Maxwell's equations in general orthogonal coordinate systems and the perfectly matched layer," *Microwave Opt. Technol. Lett.*, vol. 24, no. 1, pp. 31–34, Jan. 2000.

[5] H. Derudder, F. Olyslager, and D. De Zutter, "An efficient series expansion for the 2-D Green's function of a microstrip substrate using perfectly matched layers," *IEEE Microwave Guided Wave Lett.*, vol. 9, pp. 505–507, Dec. 1999.

[6] P. Bienstman, H. Derudder, R. Baets, F. Olyslager, and D. De Zutter, "Analysis of cylindrical waveguide discontinuities using vectorial eigenmodes and perfectly matched layers," *IEEE Trans. Microwave Theory Tech.*, vol. 49, pp. 349–354, Feb. 2001.

[7] H. Derudder, F. Olyslager, D. De Zutter, and S. Van den Berghe, "Efficient mode-matching analysis of discontinuities in finite planar substrates using perfectly matched layers," *IEEE Trans. Antennas Propagat.*, to be published.

[8] R. M. Corless, G. H. Gonnet, D. E. G. Hare, D. J. Jeffrey, and D. E. Knuth, "On the Lambert W function," *Adv. Comput. Math.*, vol. 5, no. 4, pp. 329–359, 1996.

Wide-Bandwidth Millimeter-Wave Bond-Wire Interconnects

Thomas P. Budka

***Abstract*—A new type of interconnect has been developed that significantly extends the bandwidth of fixed-length bond-wire interconnects between microwave circuits. This interconnect maximizes bond-wire length, as well as landing pad size while simultaneously extending the cutoff frequency of the interconnect. The bond-wire interconnect is treated as a five-stage low-pass filter where basic filter theory is used to develop an interconnect prototype. Microstrip interconnects are designed using electromagnetic simulators, which match a specific low-pass filter response on a 5-mil-thick (127 μm) glass substrates. The measurements indicate a return loss greater than 12 dB and an insertion loss from 0.0 to 0.3 dB from dc to 80 GHz using two 17-mil-long (432 μm) 1-mil-diameter (25 μm) ball bonds with a tolerance of $\pm$ 2 mil (50 μm). For comparison, an uncompensated interconnect with two 17-mil-long (432 μm) bond wires has 1-dB insertion loss and 10-dB return loss at 40 GHz and continues to degrade at higher frequencies.**

I. Introduction

Historically, chip-to-chip interconnects using bond wires have been analyzed as having a single electrical component: a series inductor. In order to improve the high-frequency performance of a bond-wire interconnect, efforts have usually focused on reducing the length of the bond wire and also reducing the chip-to-chip spacing. However, limitations in manufacturing require longer bond-wire lengths and wider chip-to-chip spacing to improve the yields of millimeter-wave multichip assemblies (MCAs). Therefore, the goal for millimeter-wave interconnect design is to maximize bond-wire length to improve manufacturability and maximize bond pad size so that mechanical tolerances are eased. This paper demonstrates that this is possible with a filter theory approach to interconnect design.

A single bond-wire interconnect can be treated as a single-stage low-pass filter with a fixed cutoff frequency. As more stages of the filter are added, the bandwidth of the filter increases until adding additional stages becomes inappropriate due to unacceptable filter losses. Usually low-pass filters are between three and seven stages. For this specific design example, the bond-wire interconnect is treated as a five-stage low-pass filter.

Fig. 1 displays a five-stage low-pass filter prototype with series inductors and shunt capacitors. There are well-known published tables in the literature of the relative values of the inductances and capacitances for filter design [1]. For example, if a 0.5-dB equal-ripple response is desired, then a single inductor filter would have an inductance of $0.70L$. A five-stage equal-ripple filter with the same cutoff frequency would have a center inductor of $2.54L$ and two outer inductors of $1.71L$ [2], where L is the inductance that selects the cutoff frequency of the filter. This implies that for the same cutoff frequency of the single- and five-stage filter, the center inductor in the five-stage design can have a 3.6 times higher inductance than a single inductor design. This directly translates into a 3.6 times longer bond wire for the same cutoff frequency. The ability to lengthen the bond wires is critical for high-yield assembly of millimeter-wave multichip modules.

Manuscript received June 26, 2000.

The author was with M/A-COM Research and Develpoment, Lowell, MA 01853 USA. He is now with RF Microdevices, Billerica, MA 01821 USA.

Publisher Item Identifier S 0018-9480(01)02440-1.